International Journal of Pharmaceutics 391 (2010) 221–229

Contents lists available at ScienceDirect

International Journal of Pharmaceutics

journal homepage: www.elsevier.com/locate/ijpharm

The effect of reduction of propellant mass fraction on the injection profile of metered dose inhalers

Dehao Ju [a], John Shrimpton [a,*], Alex Hearn [b]

[a] Energy Technology Group, School of Engineering Sciences, Highfield Campus, University of Southampton, Southampton S017 1BJ, UK
[b] Kind Consumer Limited, London, UK

ARTICLE INFO

Article history:
Received 5 December 2009
Accepted 2 March 2010
Available online 21 March 2010

Keywords:
Flash evaporation
Multiphase
Atomization
Model

ABSTRACT

In order to provide an improved understanding of the flow in pressurized-metered dose inhalers (pMDIs), especially monitoring the output temperature and mass flow rate to obtain maximum atomization efficiency from the available energy, a numerical model for a two phases, multi-component compressible flow in a pressurized-metered dose inhaler is presented and validated. It is suitable for testing with various formulations and different geometries for a range of pMDI devices. We validated the model against available data in the literature for a single component HFA 134a propellant, and then investigated the response of the model to other formulations containing non-volatile components. Further validation is obtained by an experiment using the dual beam method which acquired the actuation flow properties such as spray velocity and duration. The deviation of the numerical predictions for the peak exit velocity against the experimental results is 5.3% and that for effective spray duration 5.0%. From the numerical and experimental results, it is found that for the formulations with the mass fraction of HFA 134a > 80%, the effective spray duration of the pMDI is around 0.1 s. Furthermore the droplet peak exit velocity at the axial station $x = 25$ mm from the actuation nozzle decreases from 20 to 15 m/s with the reduction of the propellant (HFA 134a) from 95%. Formulations with the mass fraction of HFA 134a below 80% produce poor quality spray which is indicated from the unsteady peak exit velocity, changeable spray number density in each experimental test, and numerical simulations also confirmed the non-viability of this condition.

1. Introduction

Pressurized-metered dose inhalers (pMDIs) are widely used pharmaceutical devices designed to deliver aerosolized medication deep into the lung (Finlay, 2002). To obtain a single dose, a consumer first actuates the device by squeezing the canister into the canister casing, while simultaneously inhaling via the casing mouthpiece. Newman (2005) presents an overview of pMDI design. When a pMDI is actuated, a pressurized mixture of medication and propellant is forced out of the canister through the metering chamber (MC) and expansion chamber (EC), specially designed to ensure consistent dosing throughout the life of the device. As the mixture passes through the expansion chamber, the pressure is reduced and the propellant begins to boil. Upon leaving the expansion chamber via the nozzle, the propellant forms droplets together with the drug particles or droplets producing a spray suitable for inhalation by the consumer. This basic design remained unchanged from the introduction of pMDIs in 1956 until a switch from chlorofluorocarbon (CFC) to hydrofluoroalkane-based (HFA) propellants began in the late 1990s. The emitted spray is transient, unsteady, turbulent, three-dimensional, and multiphase.

In recent years, several researchers have attempted to use computational fluid dynamics (CFD) to model air flow as well as the transport and deposition of aerosols in the human respiratory system. Farkas et al. (2006), Jin et al. (2007), Takano et al. (2006) and Kleinstreuer et al. (2007) simulated the air flow with particle transport and tracked the releasing particles within the calculated flow domain. Their results indicated the essential role of spray velocity initial conditions on simulating delivery of pharmaceutical aerosols in the respiratory system. For flashing propellant systems, of which pMDIs are an important device class, specification of these initial conditions is problematic.

Few works have appeared in the published literature in which researchers have attempted to characterized pMDI sprays actuations experimentally. Hochrainer et al. (2005) compared the spray duration and velocity of a number of CFC-and HFA-propelled pMDIs delivering different medications. The mean aerosol velocity was reported at a distance of 10 cm from the nozzle. Three medical formulations (ipratropium bromide, ipratropium bromide + fenoterol, and fenterol), were tested in both HFA- and CFC-propelled devices. In these cases, the average velocity of each of the HFA-propelled

* Corresponding author.
E-mail address: john.shrimpton@soton.ac.uk (J. Shrimpton).

0378-5173/$ – see front matter © 2010 Elsevier B.V. All rights reserved.
doi:10.1016/j.ijpharm.2010.03.003

Nomenclature

A	cross-section area (m^2)
$c_{p/v}$	specific heat capacity at constant pressure/volume (J/(kg K))
C_d	discharge coefficient (−)
f	vapour mass fraction (vapour/gas mixture ratio) (−)
h	specific enthalpy (J/kg)
h_{fg}	latent energy of evaporation (J/kg)
H	enthalpy (J)
m	mass (kg)
$\dot{m}$	mass flow rate (kg/s)
M	molecular weight (kg/mol)
Ma	Mach number (−)
p	pressure (Pa)
q	quality of fluid (gas/mixture mass fraction) (−)
t	time (second)
T	temperature (K)
u	axial velocity (m/s)

Greek symbols

ρ	density (kg/m^3)
φ	volume fraction (−)

Subscripts

a	air
atm	atmosphere
b	background
c	critical
ds	downstream
ec	expansion chamber
g	gas
l	liquid
m	mixture
mc	metering chamber
P	propellant
r	relatively
t	nozzle throat
T	total
us	upstream

Superscripts

n	new time level
o	old time level
$*$	critical value

Universal constant

R	universal gas constant (8.314 (J/(mol K)))

pMDIs was always less than half the velocity of the corresponding CFC-propelled pMDI.

One detailed study of flash evaporation specifically in pMDIs has been conducted by Clark (1991), who attempted experiments to characterize the spray issued from a pMDI for various formulations in terms of spray mass flow rates, peak velocities, temperature, initial drop sizes and pressure variations in the MC and EC, and also developed a theoretical program for the single component flow to predict the above parameters. A range of peak exit velocities between 35 and 70 m/s were obtained at a distance of 30 mm from the actuator orifice, for propellant-134a with different orifice diameter ratios.

Dunbar (1996) provided a comprehensive theoretical and experimental analysis of the pMDI spray. They simulated the actuation flow with the single component numerical model, which

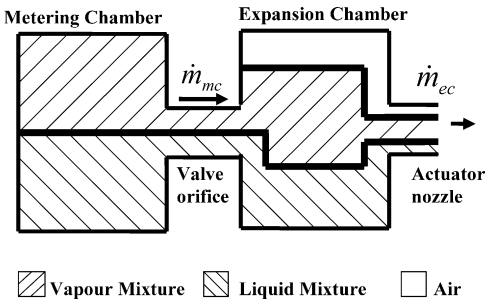

Fig. 1. Simplified actuation flow model.

indicates the multi-component actuation flow is required further study. They made experimental measurements at discrete points in the flow-field using phase-Doppler particle analysis (PDPA), which allowed droplet velocity, droplet size, and spray concentration to be measured. For the actuator orifice diameter of 0.5 mm, the axial peak exit velocity of the droplets 60 m/s was obtained at a distance of 25 mm from the actuator orifice and 15 m/s at 100 mm, with the spray duration of 0.195 s.

The direct objectives of the current work are to study the process of flashing atomization and dispersion, with a view to supporting the development of devices to deliver nicotine based solution via an aerosol that mimics the action of smoking. Preliminary findings suggest that the nicotine formulations have different volatility characteristics, and hence there is a need to investigate the multi-component two-phase flow characteristics of flashing flow, typically found in pMDIs with the aim of optimizing the process to provide very fine atomization, and to evaluate the effect of different formulations on the spray characteristics for a typical pMDI geometry.

Here, spray velocities and duration were measured using the dual laser method (Dyakowski and Williams, 1993), which utilizes the well known cross-correlation technique. Measurements were performed using HFA-propelled pMDIs, and statistical comparisons were made to study variations in performance with a number of actuations as well as for different formulations (especially with different propellant mass fraction) actuated using a single pMDI discharging into quiescent air at normal temperature and pressure.

Results of this work will be particularly useful for future researchers seeking to simulate droplet dispersion and deposition in respiratory system as well as to help validate detailed simulations of the entire pMDI spray process.

2. Methods

2.1. Mathematical modeling of a pMDI

This work is based on an earlier model, for the single component actuation flow developed by Dunbar (1996). We have improved some of the multiphase flow assumptions and added multi-component two-phase flow functionality of flashing flow as detailed in Appendix. A simplified actuation flow model is shown as Fig. 1. The geometries of the pMDI are obtained from Dunbar (1996). The volume of the metering chamber and the expansion chamber are 63.0 and 17.6 mm^3; the diameters of the valve orifice and the actuator nozzle are 0.7 and 0.5 mm, and the discharge coefficients of these are 0.61 and 0.5. These values reflect practical systems in common use.

Initially, it is a saturated vapour and liquid mixture presenting in the metering chamber. When the valve orifice opens, the fluids are released into expansion chamber. With the vapour generated, a two-phase flow is formed. The flow will be initially choked through valve orifice as the pressure difference reaches the sonic conditions. With the loss of mass in the metering chamber, the pressure

Table 1
Mass distribution of different formulations.

Net weight: 10 g	Theoretical weight (g)				
	Formula 1	Formula 2	Formula 3	Formula 4	Formula 5
Nicotine free base	0.01	0.01	0.01	0.01	0.01
Ethanol	0.1	0.2	0.4	0.8	1.5
Propylene glycol	0.39	0.79	1.59	3.19	5.99
HFA 134a	9.5	9.0	8.0	6.0	4.0

decreases and the flow become sub-critical until the pressure in the metering chamber and the expansion chamber reaches equilibrium. The gas phase coming from the metering chamber is mixed with the air residing in the expansion chamber initially, and with the incoming flow from the metering chamber, the pressure in the expansion chamber will increase until the pressure in metering and expansion chambers reaches equilibrium. At the same time, the pressure difference increases between the expansion chamber and atmosphere, initially the two-phase flow through the actuator nozzle is sub-critical, and later becomes choked. Towards the end of actuation, the flow returns to sub-critical as the pressure in the expansion chamber decreases towards atmosphere pressure.

The major assumptions of the numerical approach are:

(1) The velocity stays constant through valve orifice or actuator nozzle during each time step.
(2) Liquid phase is considered to be incompressible.
(3) In the expansion chamber, the kinetic energy discharging from the metering chamber will not be taken into account for the energy balance, which means the releasing fluid to the expansion chamber has the same stagnation temperature as that in the metering chamber.
(4) The total volume of the liquid mixture is the sum of the volume of the individual liquid components.
(5) The flow is adiabatic, which means there is no heat transfer between the fluids and the atmosphere or the device.
(6) Assume the time for evaporation is negligible, which implies the condition in the metering chamber always remains saturated.
(7) Assume there are N different liquid components and M different gaseous components.
(8) All the liquid components are miscible organic compounds, they are considered as ideally mixed.

2.2. Propellant mixtures investigated

The direct object of Kind Group Ltd. is to acquire steady, relatively slow nicotine formulation spray, which should be fine enough to be inhaled deeply into the lung and to have the appearance of cigarette smoke. In the meantime, the mass flow rate of the nicotine is required to be relatively constant. The formulations with different mass fraction of propellant HFA 134a produce the sprays with different quality, exit velocity and duration. Therefore five different nicotine formulations (Table 1) were tested in this work and thermoproperties of each component are referred to Touloukian and Makita (1970), Ray and George (1973), Perry and Green (1997), Potter and Wiggert David (1997), Fujiwara et al. (1999), Lide and David (2002), and Atkins and De Paula (2006). The formulations (Table 1) can be divided into two main parts, one is the bulk concentrate (a mixture of nicotine free base, ethanol and propylene glycol) and the other is the propellant (HFA 134a). The bulk concentrate does not easily evaporate at the room temperature and atmospheric pressure, as the vapour pressure is far below the atmospheric pressure. Conversely, the propellant is easy to evaporate to provide the propulsion for the bulk concentrate. In addition, the pure HFA 134a was used to verify the present model from the data (Dunbar, 1996).

As the actuation flow of the nicotine formula is a multi-component two-phase flow, a separated flow model is used in this study (Wallis, 1969), which means each phase of the fluid is calculated in isolation and modified by the phase quality (q: gas/mixture mass ratio). In this study, two phases are being considered, one is the liquid phase flow and the other is the gas phase flow. The flow mixture properties are calculated from the mean thermophysical properties of the fully mixed gas and liquid.

The details of the model equations may be found in Appendix. Numerically we solve a two-dimensional fifth order equation set with the time step varying from 0.0001 to 0.00001 s. There are several restrictions of the numerical model during each iteration:

(1) For the mass balance calculation at each time step, the discharging mass is always less than the original present mass, which can be expressed as: e.g. for the ith liquid component: $\dot{m}_{l,i}\Delta t \leq m^{o}_{l,i}$.
(2) For the enthalpy balance calculation at each time step, the temperature is always higher than the freezing point of each vapour component.
(3) In the expansion chamber, the partial pressure of each vapour component should not exceed the vapour pressure at the corresponding temperature; otherwise the vapour will condense to liquid phase.

2.3. Experimental measurement method

In order to verify the numerical model, and acquire the key information on the actuation simply and reliably, the dual laser beam method is applied to characterize the spray.

There are several optical methods widely used which allow for accurate characterization of particle velocities and sizes such as Phase-Doppler Anemometry (Albrecht, 2003). The dual laser beam method is a variant of the Laser Doppler Anemometry (LDA) method to determine velocity, using two parallel laser beams instead of the laser interference and two detectors are employed. Both LDA and PDA are very accurate however the optical arrangements are more complicated. Dual laser beam method is a much simpler method which also allows for spray velocity and concentration measurement, and was developed by Dyakowski and Williams (1993).

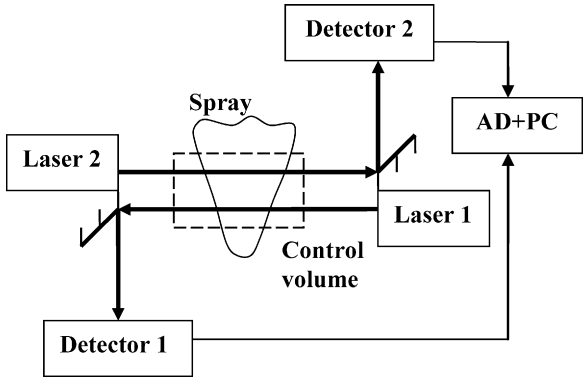

Fig. 2. Dual beam method experiment layout.

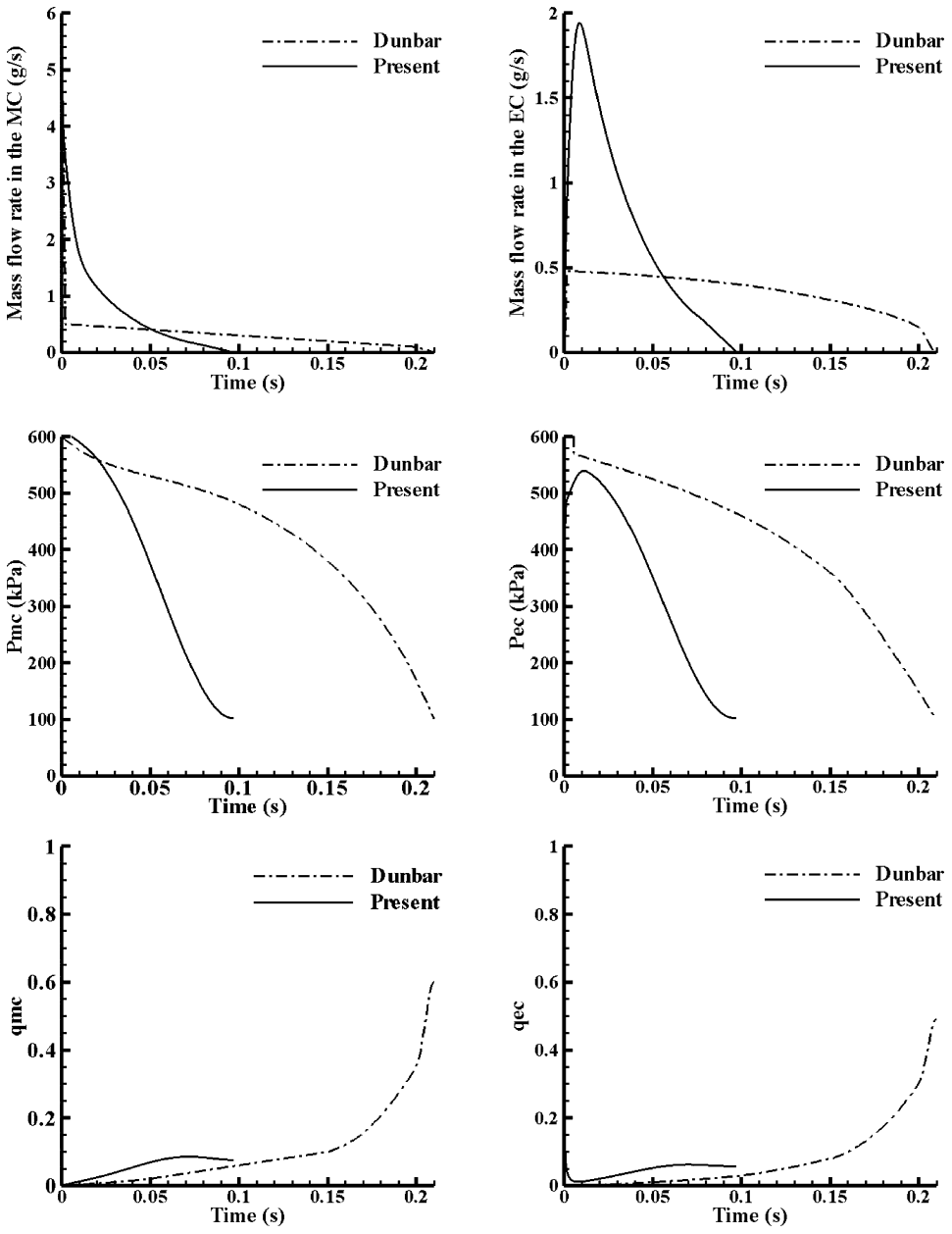

Fig. 3. Comparison of the present model results and Dunbar's data (1996).

As shown in Fig. 2, two laser beams form two control volumes across which the spray plume passes. The light intensity change of the two laser beams due to beam obscuration by the spray is detected by two photodiodes and recorded by a pc based data acquisition card (AD). When the spray passes through the first laser beam there will be a drop in voltage waveform from the correlative photodiode and similarly this will occur when it traverses the second beam. The distance between the two laser beams is known (3 mm in this work), and the time delay can be measured by the delayed signal acquired as a result of the spray taking a finite time to traverse the two beams, therefore the spray velocity could be calculated. Here, this time delay is determined by a cross-correlation procedure (Dyakowski and Williams, 1993), which represents the amount of time it takes a spray element to travel through the two laser beams.

Furthermore, assuming the spray is uniform and the droplets are spherical, the depth of the voltage drop is proportional to the surface area (of sum of the droplets) occluding the laser beam, and for a given spray mass it is an indication of the droplet sizes. Therefore a non-dimensional relative light obscuration term is introduced, which is defined by the ratio between the voltage drop when the spray transverse though the laser beams and the peak voltage when there is no spray passing. Although this cannot provide the absolute spray concentration or droplet size, it still can provide some relative measurement of spray opacity due to formulation variations. In addition the duration of the waveform gives an indication of the spread of droplet diameters present in a spray, since they will decelerate as a function of diameter.

3. Results

There are two parts to the results. First we validate the present model using numerical and experimental data with pure HFA 134a (Dunbar, 1996). Second we use the present model to simulate actuation flow with different multi-component formulations, to focus on effect of propellant mass fraction, and again, compare the

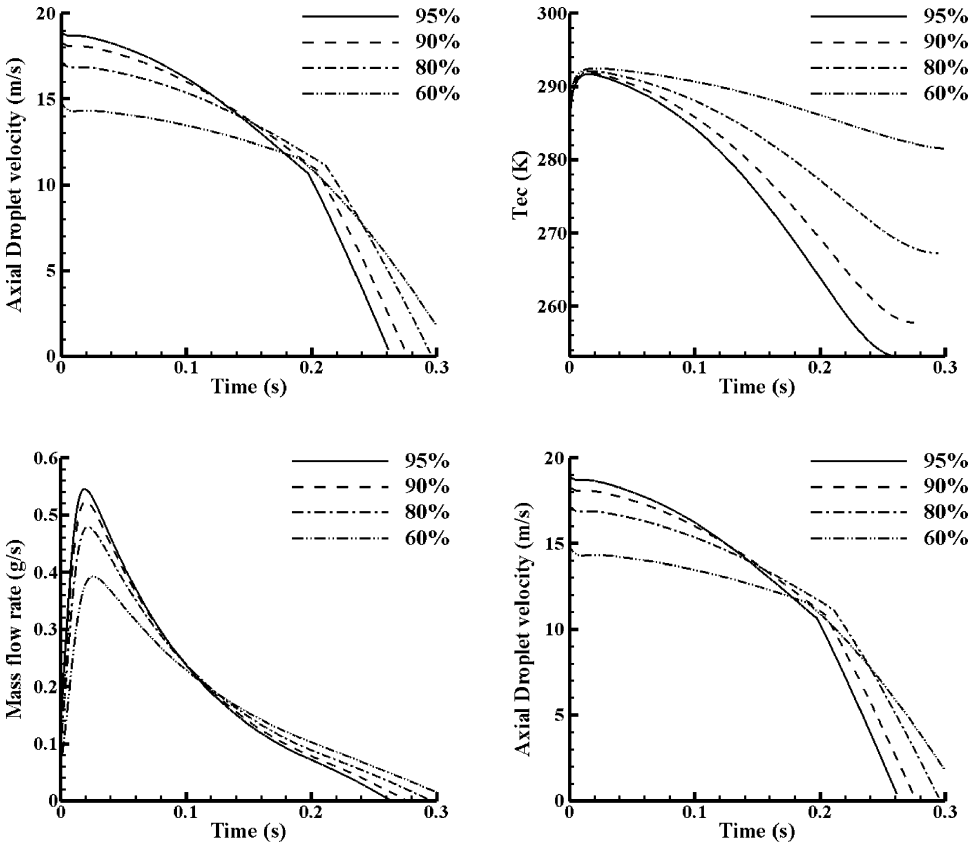

Fig. 4. Temporal variations of properties within the expansion chamber and actuation flow for the formulations with different mass fraction of propellant HFA 134a.

numerical outcomes with the experimental results. It should be noted that the nozzle orifice is 0.5 mm for the numerical tests with pure HFA 134a, to match the experimental conditions of Dunbar (1996). For the multi-component formulation numerical work, the nozzle orifice was reduced to 0.3 mm, to again match the experimental conditions.

The initial temperatures in the metering chamber and expansion chamber are the same as the ambient conditions: 293.15 K (20 °C); the pressure in the metering chamber is the vapour mixture pressure at saturated condition and room temperature. There is air residing in the expansion chamber initially, so the pressure there is atmospheric.

3.1. Result part A: validation of single component pMDI flow model

Temporal variations of the flow properties within the metering chamber and the expansion chamber are shown in Fig. 3, with the comparison to the model prediction provided from Dunbar (1996), using simple model assumptions. The actuation duration is the half of that of Dunbar (1996), which is caused by the following reasons: the definitions of the two-phase flow through the nozzle are different. In the present model, liquid and gas velocity are defined differently, while they are the same in Dunbar (1996), which leads to the gas flow rate through the nozzle in the present model is greater than Dunbar (1996), and it causes more gas lost so that more latent heat is expended from the liquid for the evaporation to reach the saturated condition. More latent heat lost results in the liquid temperature in the metering chamber decreasing more quickly than Dunbar (1996). This leads to the pressure dropping faster to atmospheric pressure, leading to a shorter actuation time. The quality of fluid in our model is below 0.1 at the end of the actuation, which means there is more fluid left in the metering chamber (roughly 10^{-6} kg left in our model while 10^{-7} kg left in Dunbar (1996)). In practice, if there is extra energy from ambient conditions, actuation time will be longer; also the evaporation process will not be instantaneous and the saturation may not be achieved at each time step as assumed in the metering chamber. There will be some heat transfer between the fluid and the inhaler case, which would 'heat up' the flow slightly and extend the actuation time. Finally the discharge coefficient of the actuator nozzle (which is assumed to be constant in the model) will be reduced by the bubble generation, cavitation flow in the expansion chamber. These factors in practice will slow down the actuation flow.

Although the actuation time from experiment provided by Dunbar (1996) is 0.195 s, the difference between experimental results and numerical results is reasonable considering the complexity of the physics.

3.2. Result part B: prediction of numerical multi-component pMDI flow model

The five different formulations (listed in Table 1) with different mass fractions of propellant used for single inhalation were tested within the typical pMDI geometry. The expansion chamber volume and the orifice diameter are kept as the same as the values of the pMDI (Dunbar, 1996), with a change of the actuation nozzle diameter to 0.3 mm to match the experimental conditions. Numerical model predictions showed that Formula 5 could not produce a spray due to the low initial pressure in the metering chamber and this was confirmed by the experiment results.

The temporal variations of the actuation flow for the formulations (Table 1) acquired from the numerical model are shown in Fig. 4. It shows that the spray durations of different formulations

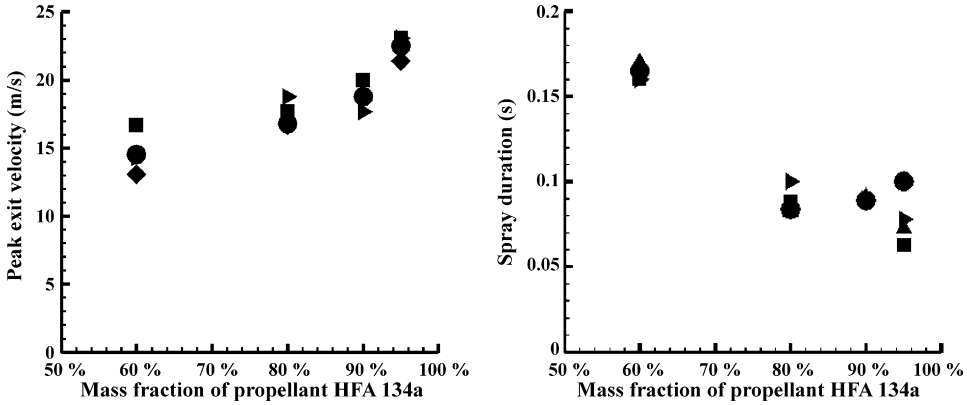

Fig. 5. Experimental analysis for the formulations with different mass fraction of HFA 134a at $x = 25$ mm.

vary slightly from each other, which are approximately 0.28 s for the whole actuation and more than twice as that of the spray generated by the 0.5 mm nozzle (0.1 s). Due to the long tail of mass distribution over time this quantity is difficult to verify experimentally. If we defined the "effective" spray duration as the period when the mass flow rate is above 0.1 g/s, it would become about 0.19 s, and around 0.12 s for the mass flow rate above 0.2 g/s. From Fig. 4, during the first 0.12 s actuation, the pressure in the expansion chamber, mass flow rate through actuation nozzle and axial droplet velocity decrease with the reduction of the propellant amount; and it could be calculated that more than 60% of the original formulations were discharged during the first 0.12 s.

In order to characterize the spray, two axial positions from the actuation nozzle were defined at $x = 25$ mm and $x = 100$ mm. The former station represents the location close to the actuator nozzle and later one is approximate distance from the actuator nozzle to the human oropharynx (Swarbrick, 2007). The spray characteristics at $x = 25$ mm obtained from the dual beam method is presented in Fig. 5, where the markers indicate that the experimental work was carried out in different ambient conditions with variation of humidity (51–71%) which do not significantly affect experimental results. The peak exit velocity near the orifice decreases with the reduction of the mass fraction of the propellant, and there is a 5.3% deviation between the numerical model and the experimental results. From the experiments, the duration of the spray at $x = 25$ mm is around 0.1 s for the formulations with the propellant above 80% and 0.15 s with 60% propellant; compared with the numerical results (Fig. 4), it implies the dual beam method could detect the spray with the mass flow rate above 0.18 g/s.

A further study on the relative spray characters at $x = 100$ mm where the human oropharynx locates is produced from the experiment, and the relative light obscuration in Fig. 6 is proportional to the surface area of the droplets occluding the laser beam. Compared to that at $x = 25$ mm, especially for the formulation with 60% propellant, the spray duration increases to 0.3 s, which is caused by the reduced pressure driving force. However, the spray durations for the formulations with more than 80% of propellant only increase up to 0.14 s. As shown in Fig. 6, the area under the curves is proportional to the total area of the laser beam cross-area occluded by the spray. Since (a) droplet area normal to the laser beam direction is proportional to the second order of the droplet diameter, (b) droplet volume is proportional to the third order and (c) formulation volume per injection is constant, the total area under the curve is inversely proportional to the mean droplet size. As a result, the ratio of the droplet diameters for the spray generated with 90%, 80% and 60% propellant, relative to the mean drop diameter of the spray with 60% propellant, is 0.64:0.73:1. Meanwhile the ratio of the bulk concentrate of the formulations with 90%, 80% and 60%

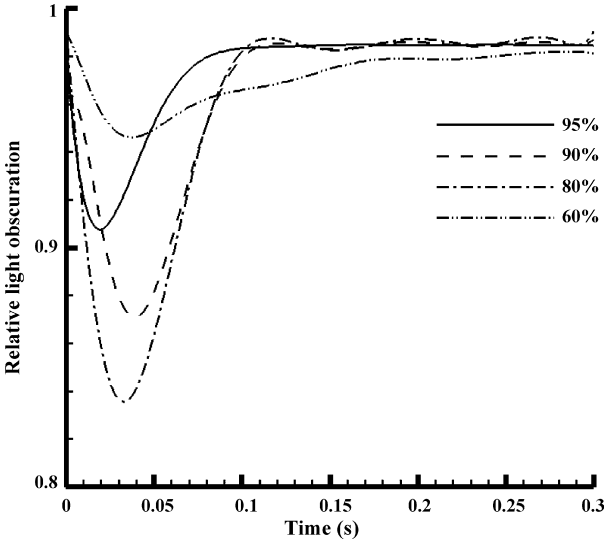

Fig. 6. Relative light obscuration for the formulations with different mass fraction of HFA 134a at $x = 100$ mm.

propellant is 0.25:0.5:1, which confirms that the above ratio is the change of the droplet diameters. Furthermore, the deepest points of the curves in Fig. 6 indicate how soon the mass of spray reach $x = 100$ mm station (oropharynx). The average time is 0.02 s for the spray with 95% propellant arriving at the point and around 0.04 s for the others. The main reason for the spray with 95% propellant arriving first is the higher vapour pressure generated in the metering chamber which produces the driving force (5 bar shown in Fig. 4). In summary, the formulations with 80% and 90% propellant seem to produce the most opaque sprays, however, the spray generated by the formulation with 95% propellant probably does not contain enough inert mass to produce a good cigarette 'smoke', since it is composed mostly of volatile HFA 134a which easily vapourises.

4. Conclusion

A multiphase, multi-component transient model of the key components of a typical metered dose inhaler has been developed and experimentally verified using the dual beam method and a range of propellant formulations.

From the numerical and experimental results, it is found that the effective spray duration of the pMDI is around 0.1 s for a formulation with the mass fraction of HFA 134a above 80%. The optimum mass fraction of propellant, to produce a 'smoke' like spray occurs in the range 80–90%. Above 90% too little inert mass is present, below 60%

and there is not enough flash evaporation to drive the atomization process.

Acknowledgments

We appreciated the technical support from Simon.R. Klitz and funding from Kind Consumer Ltd. (www.kindconsumer.com).

Appendix A. Model equations

With the reference to Solomon et al. (1985), Potter and Wiggert David (1997) and Aamir and Watkins (2000), first we define the calculation of properties of single component liquid at saturated condition in a closed vessel, the mass fraction of the vapour is calculated out as follows:

$$q = \frac{m_v}{m_T} = \frac{(\rho_l/\bar{\rho}) - 1}{(\rho_l/\rho_v) - 1} \tag{1}$$

where the mixture density of the vapour and liquid is the ratio of total mass and vessel volume:

$$\bar{\rho} = \frac{m_T}{V} \tag{2}$$

Similarly a multi-component liquid at saturated conditions is also expressed from (1), where the pure component properties should be changed to mixture properties. The liquid (l), mixture (m) density is the ratio of total mass and total volume of liquid mixture:

$$\rho_{l,m} = \frac{\sum_{i=1}^{N} m_{l,i}}{\sum_{i=1}^{N} V_i} \tag{3}$$

The vapour (v), mixture (m) pressure is calculated from the Raoult's law:

$$p_{v,m} = \sum_{i=1}^{N} x_i (p_v^*)_i \tag{4}$$

where p_v^* is the vapour pressure of the pure liquid and x_i is the mole fraction of the ith liquid component in the liquid mixture. The partial pressure of the ith vapour component is:

$$p_{v,i} = x_i (p_v^*)_i \tag{5}$$

Follows Dalton's Law, the mole fraction of *the ith* vapour component in the vapour mixture is the ratio of partial vapour pressure of each component and total vapour pressure:

$$y_i = \frac{p_{v,i}}{p_{v,m}} \tag{6}$$

The total mass of vapour of the multi-component liquid is calculated similarly from (1). The mass of each liquid and vapour component may be derived from x_i and y_i.

Extra gas (not vapour) in the metering chamber makes little difference to the change of the vapour pressure when it is low, less than 10 bar. The total pressure in the vessel, which is the sum of total vapour pressure of the liquid mixture and the partial pressure of the extra gas:

$$p_T = p_{v,m} + p_{g,m} \tag{7}$$

where total vapour pressure of the liquid mixture $p_{v,m}$ is defined from (4), and partial pressure of the extra gas is calculated from its mass as follows:

$$p_{g,m} = \frac{\sum_{j=1}^{M} m_{g,j}}{V_{v+g,m}} \tag{8}$$

where $V_{v+g,m}$ is the total volume of vapour and gas volume.

To define the two-phase fluid flow through a nozzle or orifice, we must first define the gas phase mass fraction as follows:

$$q = \frac{m_g}{m_l + m_g} \tag{9}$$

The volume fraction of gas is calculated from q as follows:

$$\varphi = \frac{V_g}{V_l + V_g} = \frac{q\rho_l}{(1-q)\rho_g + q\rho_l} \tag{10}$$

and the areas of cross-section of each phase stream are:

$$A_g = \varphi A_t \tag{11}$$

$$A_l = (1-\varphi) A_t \tag{12}$$

Similarly to the mass flow rate of the single phase flow, for the two-phase flow, the mass flow rate of each phase is defined as follows:

$$\dot{m}_g = \varphi A_t \cdot p_o \sqrt{\frac{\gamma}{RT_o}} Ma_t \left(1 + \frac{\gamma - 1}{2} {Ma_t}^2\right)^{(\gamma+1)/(2(1-\gamma))} \tag{13}$$

$$\dot{m}_l = (1-\varphi) A_t \sqrt{2\rho_l (p_{us} - p_{ds})} \tag{14}$$

and total mass flow rate is calculated as follows:

$$\dot{m}_T = \dot{m}_g + \dot{m}_l \tag{15}$$

When the flow is choked at a throat, Ma_t = 1. Assuming the incompressible liquid is dispersed as drops in the nozzle, the liquid serves noly to reduce the effective throat area, gas phase is considered to be 'choked' when the pressure reaches critical value at the throat.

A.1. Calculation of conditions for the flow in the metering chamber

In the metering chamber, the two-phase fluid remains saturated during the actuation, so the thermophysical properties for each component of both phases are the function of temperature.

Total mass in the metering chamber is the sum of the mass of each liquid, vapour components and extra gases:

$$m_{T,mc} = \sum_{i=1}^{N} m_{v,i,mc} + \sum_{i=1}^{N} m_{v,i,mc} + \sum_{j=1}^{M} m_{g,j,mc} \tag{16}$$

Total enthalpy in the metering chamber is the sum of total liquid mixture enthalpy and total gas, vapour mixture enthalpy:

$$H_{T,mc} = m_{T,l,mc} h_{l,m,mc} + m_{T,v+g,mc} h_{v+g,m,mc} \tag{17}$$

where $h_{l,m,mc}$ is the specific enthalpy at constant pressure of liquid mixture, and that of the vapour and gas mixture is $h_{v+g,m,mc}$.

The total mass flow rate for two-phase flow through valve orifice $\dot{m}_{T,mc}$ (explained below) is the mass flow rate discharging from the metering chamber to the expansion chamber. Separately, the total liquid mixture mass flow rate is shown as $\dot{m}_{l,m,mc}$, and that of vapour, gas mixture is $\dot{m}_{v+g,m,mc}$, where

$$\dot{m}_{T,mc} = \dot{m}_{l,m,mc} + \dot{m}_{v+g,m,mc} \tag{18}$$

At a new time level, the mass of each liquid component in the metering chamber after discharging to the expansion chamber is defined from the total liquid mixture mass flow rate as follows:

$$m_{l,i,mc}^{n} = m_{l,i,mc}^{o} - \phi_{i,mc} \dot{m}_{l,m,mc} \Delta t \tag{19}$$

where $\phi_{i,mc}$ is the mass fraction of each liquid component in the metering chamber and $\phi_{i,mc}\dot{m}_{l,m,mc}\Delta t$ is the discharged amount of the ith liquid.

Similarly, mass of each vapour component in the metering chamber at a new time level after discharging is:

$$m^{n}_{v,i,mc} = m^{o}_{v,i,mc} - f_{i,mc}\dot{m}_{v+g,m,mc}\Delta t \tag{20}$$

and the mass of each gas component is:

$$m^{n}_{g,j,mc} = m^{o}_{g,j,mc} - f_{j,mc}\dot{m}_{v+g,m,mc}\Delta t \tag{21}$$

where $f_{i,mc}$ is the mass fraction for each vapour of the vapour and gas mixture and $f_{j,mc}$ is the mass fraction for each extra gas of the vapour and gas mixture.

At a time point, both liquid and vapour phases reside in the metering chamber. Upon actuation, liquid must evaporate to maintain the pressure as saturated. The evaporation causes the chamber temperature decreasing as latent heat energy is expended. For a multi-component liquid, each component evaporates different amount of vapour according to its partial vapour pressure and latent heat at that temperature. Then,

The total enthalpy balance in the metering chamber can be expressed as follows:

$$\underset{A}{H^{n'}_{T,mc}} = \underset{B}{H^{o}_{T,mc}} - \underset{C}{\Delta H^{o}_{T,mc}} - \underset{D}{\text{Latent}} \tag{22}$$

where A is the total enthalpy in the metering chamber at new time step after discharging and evaporation (17); B is the total enthalpy in the metering chamber at old time step before discharging and evaporation (17); C is the enthalpy loss caused by the mass discharged through orifice valve; D is the total latent energy expended by evaporation of liquids in the metering chamber.

where the enthalpy loss is:

$$\Delta H^{o}_{T,mc} = \dot{m}_{v+g,m,mc}\Delta t \cdot h^{o}_{v+g,m,mc} + \dot{m}_{l,m,mc}\Delta t \cdot h^{o}_{l,m,mc} \tag{23}$$

and total latent energy expended is the sum of that for each component:

$$\text{Latent} = \sum_{i=1} \left(m^{n'}_{v,i,mc} - m^{n}_{v,i,mc}\right) h^{n'}_{fg,i} \tag{24}$$

where $m^{n'}_{v,i,mc}$ is mass of *the ith* vapour component after discharging and evaporation; $m^{n}_{v,i,mc}$ is mass of *the ith* vapour component after discharging but before evaporation, defined in (20).

Enthalpy balance equation provides the new time level temperature in the metering chamber.

A.2. Calculation of conditions for the flow out of the expansion chamber

As the expansion chamber is connected to the atmosphere through the actuator nozzle, there is air residing in the expansion chamber before actuation. So the extra air should be taken into account for the calculations in the expansion chamber.

The quality of fluid (gas/mixture mass fraction) in the expansion chamber is:

$$q_{ec} = \left(\frac{m_{T,v} + m_{T,g}}{m_{T,l} + m_{T,v} + m_{T,g}}\right)_{ec} \tag{25}$$

Similar to the definition of the mass flow rate for the two-phase flow through the valve orifice (21), the total mass flow rates through actuator nozzle $\dot{m}_{T,ec}$ is defined, which is the mass flow rate discharging from the expansion chamber to ambient conditions. The liquid mixture mass flow rate is expressed as $\dot{m}_{l,m,ec}$, and that of vapour, gas mixture is $\dot{m}_{v+g,m,ec}$, and is related as follows:

$$\dot{m}_{T,mc} = \dot{m}_{l,m,mc} + \dot{m}_{v+g,m,mc} \tag{26}$$

A mass balance in the expansion chamber defines the mass of fluid left after a time interval as follows:

$$\underset{A}{m^{n}_{T,ec}} = \underset{A}{m^{o}_{T,ec}} - \underset{B}{\dot{m}_{T,ec}\Delta t} + \underset{C}{\dot{m}_{T,mc}\Delta t} \tag{27}$$

At a new time level, the total mass of components in the expansion chamber is calculated from three parts from the old time level: A is the total mass already present in the expansion chamber; B is the mass discharged through actuator nozzle out to atmosphere; C is the mass discharged from metering chamber, through the valve orifice into the expansion chamber.

From above expression, the mass of each liquid component in the expansion chamber at a new time level yields:

$$m^{n}_{l,i,ec} = m^{o}_{l,i,ec} - \phi_{i,ec}\dot{m}_{l,m,ec}\Delta t + \phi_{i,mc}\dot{m}_{l,m,mc}\Delta t \tag{28}$$

Similarly the mass of each vapour component in the expansion chamber at a new time level is:

$$m^{n}_{v,i,ec} = m^{o}_{v,i,ec} - f_{i,ec}\dot{m}_{v+g,ec}\Delta t + f_{i,mc}\dot{m}_{v+g,mc}\Delta t \tag{29}$$

and the mass of each gas is:

$$m^{n}_{g,j,ec} = m^{o}_{g,j,ec} - f_{j,ec}\dot{m}_{v+g,ec}\Delta t + f_{j,mc}\dot{m}_{v+g,mc}\Delta t \tag{30}$$

Like the mass balance in the expansion chamber defined above, the total enthalpy at a new time level in the expansion chamber is also expressed from three parts:

$$\underset{A}{H^{n}_{T,ec}} = \underset{A}{H^{o}_{T,ec}} - \underset{B}{\dot{H}^{o}_{T,ec}} + \underset{C}{\dot{H}^{o}_{T,mc}} \tag{31}$$

where A is the total enthalpy of the mass resided in the expansion chamber at old time; B is the total enthalpy discharged through actuator nozzle to the atmosphere; C is the total enthalpy added in from the metering chamber, calculated from (23).

Similar as the calculations in the metering chamber, the expressions for the total enthalpy in the expansion chamber and the total enthalpy discharged through actuator nozzle could be derived from (17) to (23).

References

Aamir, M.A., Watkins, A.P., 2000. Numerical analysis of depressurisation of highly pressurised liquid propane. Int. J. Heat Fluid Flow 21, 420–431.

Albrecht, H.E., 2003. Laser Doppler and Phase Doppler Measurement Techniques. Springer, Berlin.

Atkins, P.W., De Paula, J., 2006. Atkins' Physical Chemistry. Oxford University Press.

Clark, A.R., 1991. Metered atomization for respiratory drug delivery. Ph.D. Thesis, Loughborough University of Technology.

Dyakowski, T., Williams, R.A., 1993. Measurement of particle velocity distribution in a vertical channel. Powder Technol. 77, 135–142.

Dunbar C.A., 1996. An experimental and the theoretical investigation of the spray issued from a pressurized metered-dose inhaler. Ph.D. Thesis, Institute of Science and Technology, University of Manchester.

Farkas, A., Balashazy, I., Szocs, K., 2006. Characterization of regional and local deposition of inhaled aerosol drugs in the respiratory system by computational fluid and particle dynamics methods. J. Aerosol Med. 19, 329–343.

Finlay, W., 2002. The Mechanics of Inhaled Pharmaceutical Aerosols: An Introduction. Academic Press, San Diego.

Fujiwara, K., Nakamura, S., Noguchi, M., 1999. Thermodynamic properties for R-404A. Int. J. Thermophys. 20, 129–140.

Hochrainer, D., Holz, H., Kreher, C., Scaffidi, L., Spallek, M., Wachtel, H., 2005. Comparison of the aerosol velocity and spray duration of Respimat® soft Mist inhaler and pressurized metered dose inhalers. J. Aerosol Med. 18, 273–282.

Jin, H.H., Fan, J.R., Zeng, M.J., Cen, K.F., 2007. Large eddy simulation of inhaled particle deposition within the human upper respiratory tract. J. Aerosol Sci. 38, 257–268.

Kleinstreuer, C., Shi, H.W., Zhang, Z., 2007. Computational analyses of a pressurized metered dose inhaler and a new drug aerosol targeting methodology. J. Aerosol Med. 20, 294–309.

Lide, David, R., 2002. CRC Handbook of Chemistry and Physics, 83rd edition.

Newman Stephen, P., 2005. Principle of metered-dose inhaler design. Respir. Care 50, 1177–1190.

Perry, R.H., Green, D.W., 1997. Perry's Chemical Engineers' Handbook, 7th edition.

Potter, M.C., Wiggert David, C., 1997. Mechanics of Fluids, 2nd edition. Pretice-Hall, Inc.

Ray, E.D., George, L.T., 1973. Handbook of Tables for Applied Engineering Science. CRC Press.

Solomon, A.S.P., Rupprecht, S.D., Chen, L.D., Faeth, G.M., 1985. Flow and atomization in flashing injectors. Atomisation Spray Technol. 1, 53–76.
Takano, H., Nishida, N., Itoh, M., Hyo, N., Majima, Y., 2006. Inhaled particle deposition in unsteady-state respiratory flow at a numerically constructed model of the human larynx. J. Aerosol Med. 19, 314–328.
Touloukian, Y.S., Makita, T., 1970. Specific heat: nonmetallic liquids and gases. Thermophys. Properties Matter 6.
Wallis, G.B., 1969. One-dimensional Two-phase Flow. McGraw-Hill, Inc., New York.
Swarbrick, J., 2007. 3rd edition. Encyclopedia of Pharmaceutical Technology, 4. Informa Healthcare USA, Inc.